Prototype tests for the ALICE TRD

A. Andronic[1], H. Appelshäuser[2], C. Blume[1], P. Braun-Munzinger[1], D. Bucher[3], O. Busch[1], G. Cătănescu[2,4], S. Chernenko[5], M. Ciobanu[1,4], H. Daues[1], D. Emschermann[2], O. Fateev[5], Y. Foka[1], C. Garabatos[1], T. Gunji[6], N. Herrmann[2], M. Inuzuka[6], E. Kislov[5], V. Lindenstruth[7], W. Ludolphs[2], T. Mahmoud[2], V. Petracek[2], I. Rusanov[2], A. Sandoval[1], R. Santo[3], R. Schicker[2], R.S. Simon[1], H.-K.Soltveit[2], J. Stachel[2], H. Stelzer[1], G. Tsiledakis[1], B. Vulpescu[2], J.P. Wessels[2,1], B. Windelband[2], C. Xu[2], V. Yurevich[5], Y. Zanevsky[5], O. Zaudtke[3]

[1]GSI Darmstadt, [2]PI, Universität Heidelberg, [3]IKP, Universität Münster, [4]NIPNE Bucharest, [5]JINR Dubna, [6]University of Tokyo, [7]KIP, Universität Heidelberg (for the ALICE Collaboration)

1 Introduction

The ALICE Transition Radiation Detector (TRD) [1] will be constructed to provide pion rejection of about 100 for the study of quarkonia and open charm mesons in heavy-ion collisions at LHC. An important aspect of the ALICE TRD is its capability to provide a trigger for high momentum electrons. A good position resolution of the drift chamber (DC) of about 400 μm is necessary in oder to achieve the challenging tasks of the TRD trigger [1]. Early measurements, performed with one single layer, indicated that the expected performances can be achieved [2]. Four identical prototype drift chambers (DC), with a construction similar to that anticipated for the final ALICE TRD [1], but with a smaller active area (25×32 cm^2), were constructed with the goal of measuring the multilayer performance. In addition, a real-size prototype was completed recently. They were tested in 2002 in pion/electron beams at GSI (p=1 GeV/c) and at the CERN PS (p=1 to 6 GeV/c). Below we present an overview of the CERN measurements. The final premplifier/shaper (PASA) was used for these tests. Two threshold Cherenkov detectors and a Pb-glass calorimeter are used to discriminate between electrons and pions in the beam.

2 General detector performance

In Fig. 1 we present the charge spectra for all 5 layers for pions and electrons at p=2 GeV/c. Besides small calibration constants (included), the response of the detector is identical for each layer.

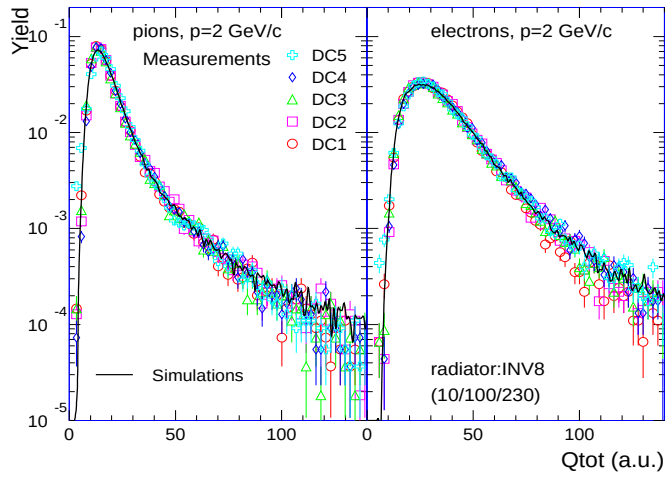

Figure 1: Charge spectra for pions and electrons at p=2 GeV/c. Symbols are data, lines are simulations.

The curves are the result of simulations, adjusted to the data with one calibration constant. The simulations reproduce the measurements well, both for pions and for electrons (a parametrization of a regular radiator was used for TR calculation).

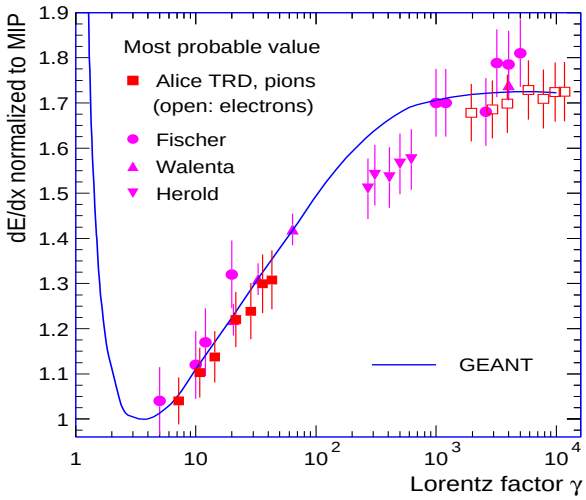

Figure 2: Relativistic rise in Xe-based gas mixtures.

In Fig. 2 we present the relativistic rise of the energy loss in our drift chambers. The curve is the result of calculations (as included in the AliRoot simulation framework), which reproduce well the measured values. The measured values for electrons (without radiator) are used to normalize the data to the simulations.

3 Pion rejection

Our radiators are sandwiches composed of polypropylene (PP) fibres and 2 sheets of Rohacell of 6 mm (INV6, AIK6) or 8 mm (INV8) thick. A carbon fibre coating of 100 μm is applied on the external sides of the Rohacell sheets (INV and AIK stand for two different manufacturers of this coating). The total thickness of a radiator is 4.8 cm. In addition, for comparison purposes, we tested pure PP fibres of 4 cm thickness.

In Fig. 3 we present the pion efficiency (the pion rejection is the inverse of this value) as a function of momentum for the three sandwich radiators and for pure PP fibres. The results without radiator are included as well. A likelihood on the measured total charge averaged over 4 layers is used to calculate the expected pion efficiency for six layers (final configuration in ALICE). A pion rejection of around 100 is achieved for any of the three coated sandwich radiators. Work is underway to improve the identification

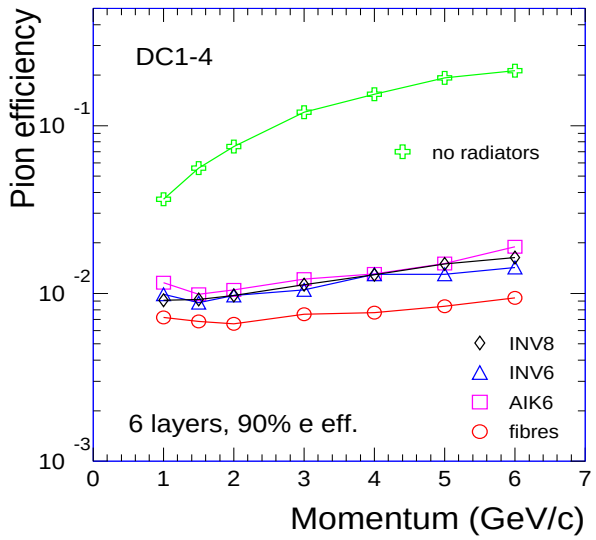

Figure 3: Radiator performance: pion efficiency as a function of momentum.

method to provide a safety factor for the expected degradation of the performance in high-multiplicity events.

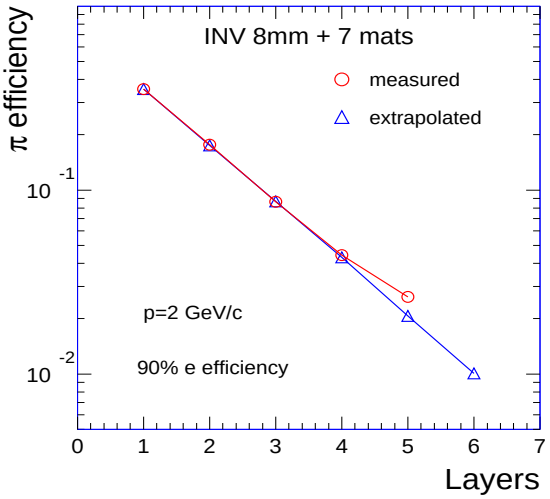

Figure 4: Multilayer performance: pion efficiency as a function of the number of layers.

In Fig. 4 we present the pion efficiency as a function of the number of layers considered in the likelihood. Measured data (open circles) are compared to the results of calculations using as inputs the measured single layer performance. As expected, the agreement between the two cases is very good, with the exception of the fifth layer, the real-size detector, for which the degradation of the performance is attributed to its larger noise during the measurements.

4 Position resolution

For each time sample, the charge sharing among neighboring pads provides information about the displacement of the ionisation relative to the pad center. The position resolution is extracted by performing a straight-line fit of the reconstructed trajectory of a particle within one chamber. The point resolution is calculated from the width of the distribution of the residuals of the reconstructed points to the fit. The width σ of a gaussian fit to the distribution of reconstructed angles measures the angular resolution. Tails of detector signal contribute to a deterioration of the position resolution. To minimize this, a tail cancellation was performed, similar to the one envisaged for the final detector [1]. The following results are for the beam momentum of 3 GeV/c, for the small-size detectors.

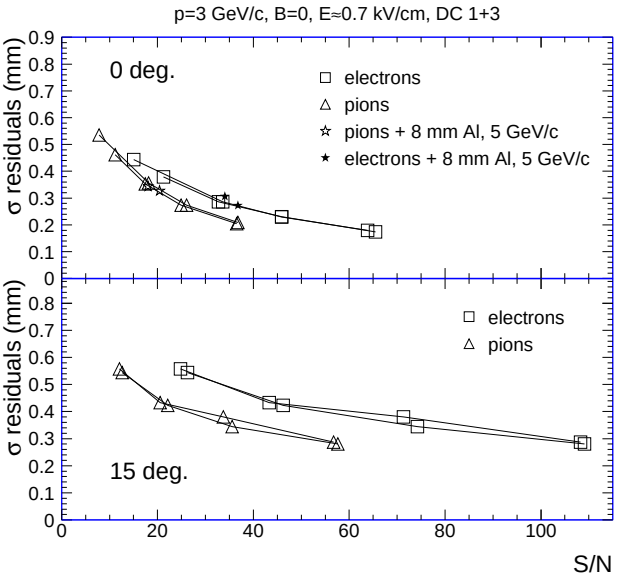

Figure 5: Position resolution for electrons and pions as a function of signal-to-noise ratio for perpendicular beam incidence and 15° chamber tilt.

In Fig. 5, we present the point resolution for 0° and 15° tilt of the DC with respect to the normal beam incidence. The variance σ of the residuals is shown for pions and electrons as a function of the signal-to-noise ratio, S/N. Different values of S/N were obtained varying the gas gain via the anode voltage. For electrons, stronger ionisation results in higher values of S/N for a given gas gain. At given S/N, the resolution is slightly worse for electrons compared to pions, presumably due to Bremsstrahlung in the detector gas and radiator. At the anticipated operational point of S/N≈30 a resolution of well below 400 μm is reached. We carried out dedicated runs introducing an aluminium plate of 8 mm thickness, corresponding to a radiation length $X/X_0 \approx 9\%$, in the beamline in front of the detectors. This dummy material simulates, in an exagerated way, the effect of the detectors in front of TRD in the final ALICE setup. These measurements were carried out at beam momentum of 5 GeV/c. The results are included in Fig. 5. For both electrons and pions, the effect of the material is negligible. Measurements in the presence of magnetic field are under evaluation.

In Fig. 6 we investigate the angular dependence of the position reconstruction performance. Point and angular

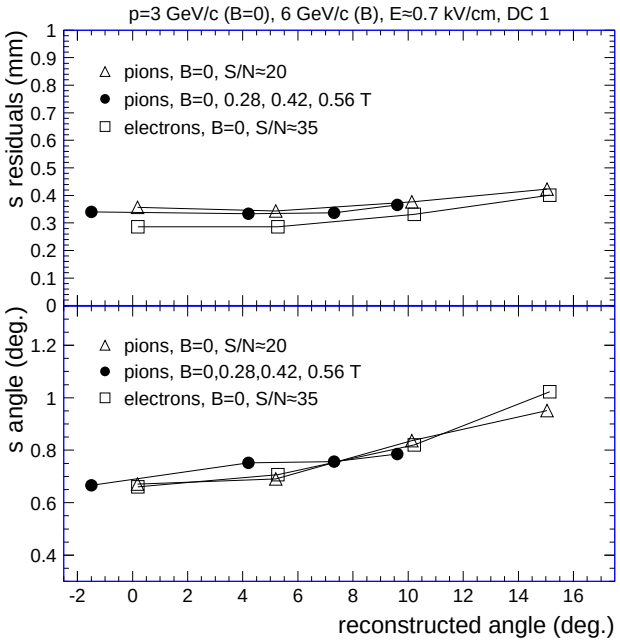

Figure 6: Point and angular resolution as a function of reconstructed angle for different values of the magnetic field.

resolution are shown for different values of incident angle relative to the normal incidence, with and without applying a magnetic field (in the ALICE setup the nominal value is B=0.5 T). For field-free runs, the reconstructed angle corresponds to the chamber tilt. If a magnetic field is applied, the Lorentz angle of the drifting electrons with respect to the electric field lines is superimposed on the beam incidence. For both electrons and pions, the point resolution is between 300 and 500 μm, irrespective of the B value, and the angular resolution is below 1°.

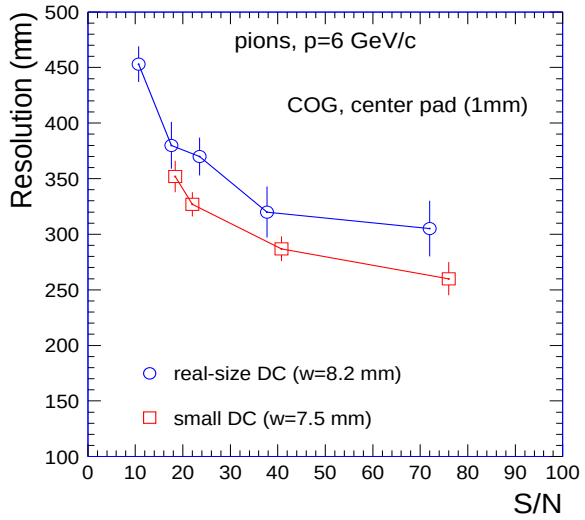

Figure 7: Position resolution as a function of S/N: comparison of small and big chambers.

Figure 7 shows a comparison of point resolution for the small and big prototypes. These results were obtained with respect to a silicon strip detector and, as a consequence, they include the effect of multiple scattering in the intervening material. To minimize this contribution, the measurements were carried out at the momentum of p=6 GeV/c. The big DC has similar position resolution compared to the small one. The differences can be accounted for by the larger pad width (8.2 mm compared to 7.5 mm for small DC).

5 TR spectrum

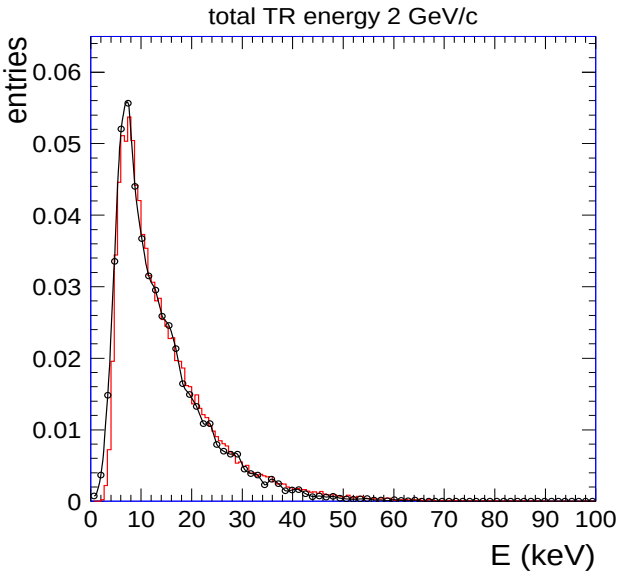

Figure 8: TR spectrum at p=2 GeV/c. Circles: measured values, histogram: simulations.

The transition radiation (TR) spectrum produced by radiators is usually measured superimposed on the energy loss of the electrons. Knowledge of TR spectrum is important as input in our simulations of the TRD. We performed dedicated measurements, placing the radiator 80 cm in front of DC and using a magnetic field to deflect the beam. To minimize TR absorption, a He-pipe was used between radiator and DC. In Fig. 8 we present an example of the measured total TR spectrum for the momentum of 2 GeV/c. Simulations using a parametrization for a regular radiator reproduce well the measured spectrum for a given momentum. Similar measurements were performed for p=1.5, 3 and 4 GeV/c.

In summary, the measured data with prototype detectors demonstrate that the needed performance of ALICE TRD can be achieved, both in terms of pion rejection and position resolution. These measurements help to freeze the final detector parameters, in time for the start of mass production by mid-2003.

References

[1] ALICE TRD Technical Design Report, CERN/LHCC 2001-021 (2001), *http://www.gsi.de/∼alice/trdtdr*

[2] A. Andronic et al., IEEE Trans. Nucl. Sc., vol. 48, 1259 (2001) [nucl-ex/0102017]